MARCH 1981 PPPL-1766
UC-20b,g

MHD STABILITY OF VERTICALLY ASYMMETRIC TOKAMAK EQUILIBRIA

BY

H. E. DALHED, R. C. GRIMM,
AND J. L. JOHNSON

PLASMA PHYSICS LABORATORY

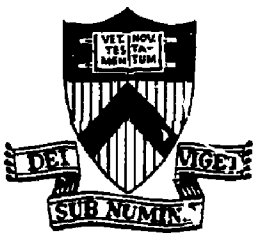

PRINCETON UNIVERSITY
PRINCETON, NEW JERSEY

This work supported by the U.S. Department of Energy Contract No. DE-AC02-76-CHO-3073. Reproduction, translation, publication, use and disposal, in whole or in part, by or for the United States Government is permitted.

MHD Stability of Vertically Asymmetric Tokamak Equilibria

H. E. Dalhed,* R. C. Grimm, and J. L. Johnson+

Plasma Physics Laboratory, Princeton University

Princeton, New Jersey 08544

Abstract

The ideal MHD stability properties of a special class of vertically asymmetric tokamak equilibria are examined. The calculations confirm that no major new physical effects are introduced and the modifications can be understood by conventional arguments. The results indicate that significant departures from up-down symmetry can be tolerated before the reduction in β becomes important for reactor operation.

I. INTRODUCTION

Recent progress with tokamaks has led to the design[1] of larger devices which can demonstrate long-time confinement of a high density hot plasma and allow the study of associated engineering problems. These designs all include some form of divertor operation for impurity control and helium ash removal. The most obvious scenario involves a double null poloidal divertor, but for a number of reasons, including that of making optimal use of the region inside the toroidal field coils, a single null poloidal divertor is attractive. The magnetohydrodynamic equilibrium of such a configuration will not have mirror symmetry about a central plane and it is natural to consider the consequences of this on the attainable β-values. However, this loss of symmetry complicates the study of the equilibrium and stability properties of the tokamak.

It is the purpose of this work to address a small part of this problem. We limit our study to the effect on magnetohydrodynamic stability of rotating a purely elliptic plasma cross section away from the vertical axis. This admittedly narrow model can indicate the nature of the problems introduced by the loss of symmetry without introducing the complexity associated with the change of the many possible plasma and cross-sectional parameters. It fits into and supplements an earlier survey[2] of MHD stability and forms the basis for developing tools and techniques for studying more complicated configurations. Most of all, by working with this straightforward model, we can gain insight which is necessary in order to interpret results from more complete studies.

The results reported in this work were all obtained after making minor modifications to various previously developed codes which have been used

extensively at the Princeton Plasma Physics Laboratory to study MHD equilibria and stability. The equilibria were generated by an adaptation of our free boundary tokamak equilibrium code[3] which allows the currents in external coils to be automatically adjusted to make the shape of the plasma boundary fit a prescribed contour. The stability of these equilibria to ballooning modes in the large toroidal mode number limit was carried out with a version of the BALLOON code.[4] Low toroidal mode number instabilities were computed with the PEST code.[5] When the equilibrium does not possess up-down symmetry it is necessary to allow the Fourier components of the displacement vector to be complex. To represent unstable modes with a similar numerical accuracy to that obtained in previous studies of up-down symmetric systems thus requires the computation of a matrix representing δW which has twice the rank. Similarly, the accurate calculation of the perturbed vacuum potential energy requires the evaluation of a complex (rather than purely real) scalar potential for the perturbed vacuum field. Consequently, the calculations performed here required significantly more computational resources than what was needed in previous work.

We describe the equilibrium sequences used in this study in Section II and then discuss axisymmetric ($n = 0$) instabilities, internal modes, and free boundary modes in the following Sections III, IV, and V. Interpretations and conclusions are given in Section VI.

II. EQUILIBRIUM SEQUENCES

In order to limit the parameter variations we utilized the conducting-wall boundary feature of the PEST equilibrium code.[3] In all our calculations we use a pressure distribution given by[6]

$$p(\Psi) = \beta_J p_o' \left\{(\Psi - \Psi_a) - \frac{\alpha}{2}\left[(\Psi - \Psi_o)^2 - (\Psi_a - \Psi_o)^2\right]\right.$$

$$\left. - \frac{[1 - \alpha(\Psi_a - \Psi_o)]}{(\ell + 1)(\Psi_a - \Psi_o)^{\ell}}\left[(\Psi - \Psi_o)^{\ell+1} - (\Psi_a - \Psi_o)^{\ell+1}\right]\right\} \qquad (1)$$

with β_J a measure of the poloidal beta of the equilibrium, Ψ_a and Ψ_o the values of the poloidal flux at the plasma boundary and magnetic axis, and p_o', α, and ℓ adjustable parameters. For the base case the toroidal magnetic field function is given by

$$q\frac{dq}{d\Psi} = \left(\frac{1}{\beta_J} - 1\right) R^2 \frac{dp}{d\Psi} \qquad (2)$$

with R a radius near the magnetic axis at which the vacuum toroidal field is defined. We specify the boundary of the plasma in the base case equilibrium to be an ellipse with major axis in the Z direction. This case is described in Table 1. The configuration is similar to those of the parameter study of Todd et al.[2] The major difference is in the adoption of a more complicated pressure and toroidal field function profile which makes the current gradient small near the plasma boundary and reduces the severity of kink modes.

In this study we consider two different equilibrium sequences, each associated with a rigid rotation θ_o of the major axis of the elliptic plasma boundary with respect to the vertical axis. Thus, for the base case, $\theta_o = 0^o$, the ellipse is standing; for $\theta_o = 90°$, the major axis of the ellipse points outward. For the first sequence we keep the pressure distribution $p(\Psi)$ and the shape of the toroidal field function $g(\Psi)$ fixed by Eqs. (1) and (2), but adjust the magnitude of $q\frac{dq}{d\Psi}$ to keep the same total current. This clearly allows the safety factor $q(\Psi)$ to change with the rotation. For the second

sequence we use Eq. (1) to maintain $p(\Psi)$ and keep the safety factor $q(\Psi)$ the same as in the base case. In this sequence, we additionally require that the internal toroidal and poloidal magnetic fluxes remain constant so that the current distribution changes with θ_o. The first sequence, in which the total current is preserved, should provide a good comparison for studies of axisymmetric modes. The second sequence maintains the global shear and thus should be more instructive for discussion of internal and kink modes. As θ_o increases to 90° in the q-conserving sequence with constant total current, the safety factor on axis, q_o, decreases from 1.20 to 1.00 while that at the boundary, q_a, increases from 3.14 to 4.05. This results in a significant increase in the local shear. Shear is conserved in the constant q sequence, but the total current is increased from 2.0 MA for the base case to 2.3 MA at $\theta_o = 90°$. Surprisingly, although the procedures for generating the two sequences are quite different, their equilibrium and stability behavior are remarkably similar. The change in shape of the magnetic surfaces as a function of θ_o and the location of the magnetic axis are shown in Fig. 1 for the constant q sequence. The difference between these results and those for the constant-q case could not be seen if the analogous figures were superimposed.

Each of the equilibria obtained by rotating the base case represents a starting point for a series that must be generated to study the stability properties. For each of these equilibrium cases we constructed a flux-conserving sequence[7] by increasing the parameter β_J, keeping the shape of $p(\Psi)$, the function $q(\Psi)$, the total internal poloidal and toroidal magnetic fluxes, and the boundary shape fixed. Each point of the stability investigation then consisted of determining the eigenfunction and the growth rate, in each case converged to zero mesh size,[8] for a series of β values and then extrapolating to zero growth rate to obtain a critical β.

III. AXISYMMETRIC (n = 0) MODES

It has long been realized that the shape of the plasma in a tokamak is closely related to the magnetic field index ($\partial \ln B_z / \partial \ln X$) of the vacuum toroidal field.[9] From this it is easy to predict that a plasma with a prolate cross section should be unstable with respect to a vertical perturbation and that too much oblateness should lead to an inward or outward shifting instability. Since it has been shown that passive stabilization can control these modes, most studies of them have not attempted to provide absolute stability but to limit growth rates.

Since these modes are usually understood to be associated with the attraction between the ohmic current in the plasma and that in the external circuitry which provides the shaping, it is reasonable to assume that they do not depend sensitively on the pressure and that the most meaningful study of the effect of cross-section rotation would be with the same current. Thus we investigate the $\beta_J = 1$ equilibria of our $q(\Psi)$ conserved sequence. Plots of the unstable perturbations and the growth rate as a function of θ_o are given in Fig. 2. We observe that the growth rate starts to decrease with rotation, reaching a minimum near $\theta_o = 60°$. It can be seen in Fig. 1 that the asymmetry introduces some triangularity into the magnetic surfaces. It is possible that this can help alleviate the destabilization due to ellipticity. In the calculations of Fig. 2 we did not include the effects of flux conservation in the vacuum regions associated with Lust-Martensen terms[5] which should provide additional stabilization. We have seen some improvement which can be interpreted as passive feedback stabilization[10] when incorporating these terms. Since these results have only qualitative significance we did not use the computer time necessary to converge them to zero mesh size. This study

indicates that this type of asymmetry actually simplifies the feedback stabilization problem.

IV. INTERNAL MODES

Most MHD instability studies start by considering the localized modes where destabilizing forces associated with an average field line curvature cannot be balanced by field line shear. For all the equilibria considered here, the Shafranov shift is large enough to provide favorable average curvature so that the localized criteria for stability[11] of both ideal and resistive modes are satisfied.

The importance of internal, fixed boundary instabilities was appreciated when it was recognized that low-n ballooning modes were not radially localized, but developed channels that connect the center of the plasma to the outer region.[12] Since such modes exist even with the perturbation vanishing at the plasma edge, it would be difficult to stabilize them with external feedback control. Significant understanding has recently been obtained from high-n models where the equations for the different magnetic surfaces separate and analytic progress can be made.[13-15] For this reason most studies of internal modes have concentrated on $n = 3$ modes to investigate the nonlocalized behavior and $n \to \infty$ modes to estimate beta limits.

The flux-conserving sequence provides a good comparison for determining the effect of rotation of the axis on internal modes. The results of such a study are summarized by the solid curves in Fig. 3 where critical β for stability with respect to $n = 3$ and $n \to \infty$ modes are given as functions of θ_o. We note that substantial rotation can occur before there is a significant reduction of the critical beta. Eigenfunctions for the most unstable $n = 3$

mode are given in Fig. 4. Comparison of the Fourier components of the modes for the $\theta_o = 0°$ and $\theta_o = 45°$ cases indicates that the mode structure is not radically altered. Thus it is reasonable to conclude that no new physical effects are introduced with this asymmetry so that our intuition based on previous parametric investigations can be trusted.

Several interesting observations emerged from our studies of the unstable internal modes as β is increased. As is well known, for sufficiently high pressure the magnetic axis is pushed out very close to the plasma surface and flux conservation leads to very large poloidal magnetic fields. Thus the connection length is shortened and we obtain a second region of stability with respect to $n = 3$ internal modes.[4,16,17] As can be seen from Fig. 3, rotation of the elliptic axis lowers the critical β at which instability occurs. It lowers even more the value of β at which the second stable region sets in.

The second observation concerns the shift of the eigenfunction in the transformed θ coordinate used in the usual ballooning formalism. For all the equilibria considered in this study, we found no shifted origin larger than approximately 0.1π. The largest shifts occurred near marginal stability and were found to be a decreasing function of β. Even though these shifts appear to be small, we feel that care must be exercised when extrapolating the $n \to \infty$ growth rates to obtain critical beta values.

V. FREE-BOUNDARY MODES

Most studies of free-boundary modes are complicated by the fact that kink modes depend sensitively on the shape of the toroidal current profile, especially near the plasma surface. The choice of $p(\Psi)$ and $g(\Psi)$ associated with Eqs. (1) and (2) makes both the current and its magnetic surface

derivative vanish for our base case. They remain small even for the q-conserving sequence. Thus our study of free-boundary modes is primarily concerned with the effect of relaxing the constraint on the perturbation ξ at the plasma-vacuum interface on pressure driven modes, rather than with kink mode behavior. Thus it is both reasonable and convenient to carry out our investigation using the q-conserving sequence.

The results of the study are summarized by the dashed curves in Fig. 3 where it is shown that, just as for the fixed-boundary modes, the critical β for free-boundary instabilities shows little degradation at first, but then falls significantly with θ_o. The fastest growing $n \approx 1$ mode is shown in Fig. 5. The behavior of the perturbations is quite similar to what we saw before, but with some extension into the vacuum region.

In these calculations with the q-conserving sequence there is an increase in the total current by 10%. Studies using a q-conserving sequence with constant total current give very similar results, indicating that these free boundary modes are indeed strongly pressure driven.

VI. DISCUSSION

Although limited in scope, this study indicates that if required for engineering or divertor design considerations, significant departure from up-down symmetry can be imposed in a tokamak without serious deterioration of the MHD equilibrium and stability properties. It is useful to observe that for this model the changes that occur in the significant equilibrium parameters, location of magnetic axis, shear, etc., are somewhat insensitive to the different equilibrium sequences we investigated. This gives some confidence that the results are not peculiar to a specific model.

The results from the investigation of the effect of rotating the cross section on axisymmetric modes are encouraging. Since the externally imposed fields are more complex, one might have expected that the axisymmetric modes would be worsened. The fact that the growth rate is actually reduced by some rotation indicates that design for feedback control could be simpler than for a symmetric device.

For this model, the critical betas for both internal and free-boundary modes were lowered by the introduction of asymmetry, primarily because the change in shape of the surfaces lengthens the connection length in the region of unfavorable curvature. The outward shift of the magnetic axis with increasing beta is also enhanced, leading to a decrease in the critical beta for the onset of the second stable region for internal modes. Probably the most significant inference that can be made from this work is that relatively large rotations can be imposed before significant deterioration sets in.

As an application of this work we have done some design studies of a modification of the Princeton Poloidal Divertor Experiment to provide a single divertor and make better use of the volume in the vacuum vessel. A reasonably shaped plasma cross section with only a small asymmetry can be obtained, even with the diverted region moved out into an easily accessible part of the vacuum vessel. Although detailed studies of these equilibria have not been completed, preliminary indications are that MHD stability problems will not be serious.

Clearly this study is very limited in that we carefully designed our program to provide as little parameter variation in the sequences as possible. It has always been appreciated that a D-shaped cross section with some triangularity is much superior to the purely elliptical one considered here and that adjusting the triangularity as we change the orientation would

dramatically improve the stability. Studies in this direction are especially called for. As in the earlier parameter study work, we have made no attempt to maximize β, but we have restricted our efforts to an attempt to clarify the behavior of these modes as a single parameter is changed. We feel that these studies provide a foundation for future work.

ACKNOWLEDGMENT

This work was performed under DOE contract no. DE-AC02-76-CH03073 with Princeton University. Most of it was accomplished as part of a Ph.D. dissertation submitted by one of us (H.E.D.) to the University of Wisconsin. Appreciation must be expressed to Dr. G. A. Emmert for his interest and encouragement. We also thank Drs. M. Okabayashi and D. M. Meade for their support and understanding which enabled this effort to be completed. We are indebted to them and to the Princeton MHD group, with special thanks to Drs. M. S. Chance, R. L. Dewar, and A. M. M. Todd, for helpful discussions and assistance.

REFERENCES

* Now at Lawrence Livermore National Laboratory

+ On loan from Westinghouse Research and Development Center

1. INTOR, International Tokamak Reactor, Zero Phase, International Atomic Energy Agency, Vienna, 1980.
2. Todd, A. M. M., Manickam, J., Okabayashi, M., Chance, M. S., Grimm, R. C., Greene, J. M., and Johnson, J. L., Nuclear Fusion, 19 (1979), 743.
3. Johnson, J. L., Dalhed, H. E., Greene, J. M., Grimm, R. C., Hsieh, Y. Y., Jardin, S. C., Manickam, J., Okabayashi, M., Storer, R. G., Todd, A. M. M., Voss, D. E., and Weimer, K. E., J. Comput. Phys. 32 (1979) 212.
4. Greene, J. M., and Chance, M. S., Nuclear Fusion (in press).
5. Grimm, R. C., Greene, J. M., and Johnson, J. L., in Methods in Computational Physics, "Computer Applications to Controlled Fusion Research" (J. Killeen, B. Adler, S. Fernbach, and M. Rotenburg, Eds., Academic Press, N.Y. 1976) Vol. 16, p. 253.
6. Dory, R. A., and Peng, Y.-K. M., Nuclear Fusion 17 (1977) 1.
7. Clarke, J. F., and Sigmar, D. J., Phys. Rev. Lett. 38 (1977) 40.
8. Chance, M. S., Greene, J. M., Grimm, R. C., Johnson, J. L., Manickam, J., Kerner, W., Berger, D., Bernard, L. C., Gruber, R., and Troyon, F., J. Comput. Phys. 28 (1978) 1.
9. Greene, J. M., Johnson, J. L., and Weimer, K. E., Phys. Fluids 14 (1971) 671.
10. Jardin, S. C., Phys. Fluids 21 (1978) 1851.

11. Glasser, A. H., Greene, J. M., and Johnson, J. L., Phys. Fluids 18 (1975) 875.

12. Todd, A. M. M., Chance, M. S., Greene, J. M., Grimm, R. C., Johnson, J. L., and Manickam, J., Phys. Rev. Lett. 38 (1977) 826.

13. Dobrott, D., Nelson D. B., Greene, J. M., Glasser, A. H., Chance, M. S., and Frieman, E. A., Phys. Rev. Lett. 39 (1977) 943.

14. Coppi, B., Phys. Rev. Lett. 39 (1977) 939.

15. Connor, J. W., Hastie, R. J., and Taylor, J. B., Phys. Rev. Lett. 40 (1978) 396.

16. Coppi, B., Ferreira, A., and Ramos, J. J., Phys. Rev. Lett. 44 (1980) 990.

17. Monticello, D., Park, W., Jardin, S. C., Chance, M. S., Dewar, R. L., White, R. B., Grimm, R. C., Manickam, J., Strauss. H. R., Johnson, J. L., Greene, J. M., Glasser, A. H., Kaw, P. K. Rutherford, P. H., and Valeo, E. J., in Proceedings of the Eighth International Conference on Plasma Physics and Controlled Nuclear Fusion Research, Brussels, 1980, (International Atomic Energy Agency, Vienna, 1980).

Table 1

Plasma parameters for the base case

Major radius		2.4 m.
Minor radius		0.55 m.
Ellipticity (b/a)		1.5
Angle of rotation θ_o		0°
Total toroidal current I_p		2.0 MA.
Vacuum toroidal field at 2.48 m.		5.2 T.
Average minor radius <a>		0.68 m.
Average major radius <R>		2.301 m.
Aspect ratio A = <R> / <a>		3.349
Volume		21.47 m^3
Safety factor q on axis q_o		1.20
Safety factor q at limiter q_a		3.14
Peak pressure p_o		4.53×10^5 N/m^2
Magnetic axis location X,Z		2.47 m., 0.0 m.
Profile parameters:	β_j	1.0
	p'_o	-0.22
	α	0.192
	ℓ	4
Total poloidal magnetic flux		4.31 W.
Total toroidal magnetic flux		7.76 W.
Poloidal beta β_p		1.0
Total beta β_o (based on B_o)		1.23%

Figure Captions

Fig. 1. Flux contours for equilibria at $\theta_o = 0°$, $\theta_o = 45°$, and $\theta_o = 90°$. The $\theta_o = 0°$ equilibrium corresponds to the base case described in Table 1; the other equilibria are related to this base case by a flux conserving or p/q rotation. The location of the magnetic axis for the flux conserving rotation starting from the base case is also shown. The abscissa and ordinate are given by

$\tilde{X} = [X - X(\theta_o = 0°)]/[X(\theta_o = 90°) - X(\theta_o = 0°)]$,

$\tilde{Z} = Z/Z(\theta_o = 45°)$.

Axis locations for given angles of rotation are labeled along the curve by the angle of rotation in degrees. The magnetic axis for the base case is $X(\theta_o = 0°) = 2.47$ m, $Z(\theta_o = 0°) = 0.0$;

for $\theta_o = 45°$, $X(\theta_o = 45°) = 2.54$ m, $Z(\theta_o = 45°) = 0.065$ m;

and for $\theta_o = 90°$ the axis is $X(\theta_o = 90°) = 2.59$ m, $Z(\theta_o = 90°) = 0$.

Fig. 2 Projections of the eigenmode $\underset{\sim}{\xi} \cdot \nabla\psi$ as a function of X and Z for the n = 0 (toroidal mode number) axisymmetric mode for rotations of $\theta_o = 0°$ (base case), $\theta_o = 45°$, and $\theta_o = 90°$. The equilibria all have the same pressure profile, toroidal field profile, and discharge current as described by Eqs. (1) and (2) with the parameters specified in Table 1. The vacuum is assumed to have infinite extent. The perturbation is seen to align itself along the major semiaxis of the cross section of the plasma. The growth rate as a function of angle of rotation with the growth rates normalized to the poloidal Alfvén frequency. It reaches a minimum at a rotation of approximately 60°.

Fig. 3 Critical β^* values for the n = 1 and n = 3 free boundary and the n = 3 and n→∞ internal modes as functions of the angle of rotation. The equilibria are related to the base case (Table 1) by a flux-conserving or p/q rotation. The free-boundary cases are assumed to be surrounded by a vacuum of infinite extent, while the internal mode cases are assumed to have a tightly fitting perfectly conducting wall on the plasma limiting surface. The critical β^*'s are extrapolated using 3 finite growth rates, each of which is numerically converged to "zero" mesh spacing by using 49 and 65 surfaces, and 15, 19, and 21 Fourier components. The equilibria used were numerically computed on an X-Z grid with 65 grid points in each direction; the numerical solutions were converged to a relative accuracy of 10^{-4}.

Fig. 4 Eigenmode projection $\underset{\sim}{\xi}\cdot\nabla\psi$ and its Fourier components for the n = 3 internal mode. (Top) Equilibrium at $\theta_o = 0°$. The growth rate is $\omega^2 = -3.2 \times 10^{-2}$. The equilibrium is connected to the base case by a flux-conserving pressure increase to $\beta^* = 3.87\%$. (Bottom) $\theta_o = 45°$. In this case, the growth rate is $\omega^2 = -1.9 \times 10^{-2}$. The equilibrium is connected to the base case by a flux-conserving rotation to $\theta_o = 45°$, and then a flux-conserving pressure increase to $\beta^* = 2.52\%$.

Fig. 5 Eigenmode projection $\underset{\sim}{\xi}\cdot\nabla\psi$ and its Fourier components for the n = 1 free-boundary mode. (Top) Equilibrium at $\theta_o = 0°$. The growth rate is $\omega^2 = -1.12 \times 10^{-2}$ with $\beta^* = 3.15\%$. (Bottom) $\theta_o = 45°$. The growth rate is $\omega^2 = -1.03 \times 10^{-2}$; $\beta^* = 1.41\%$. The equilibria are obtained in the manner described for Figure 4.

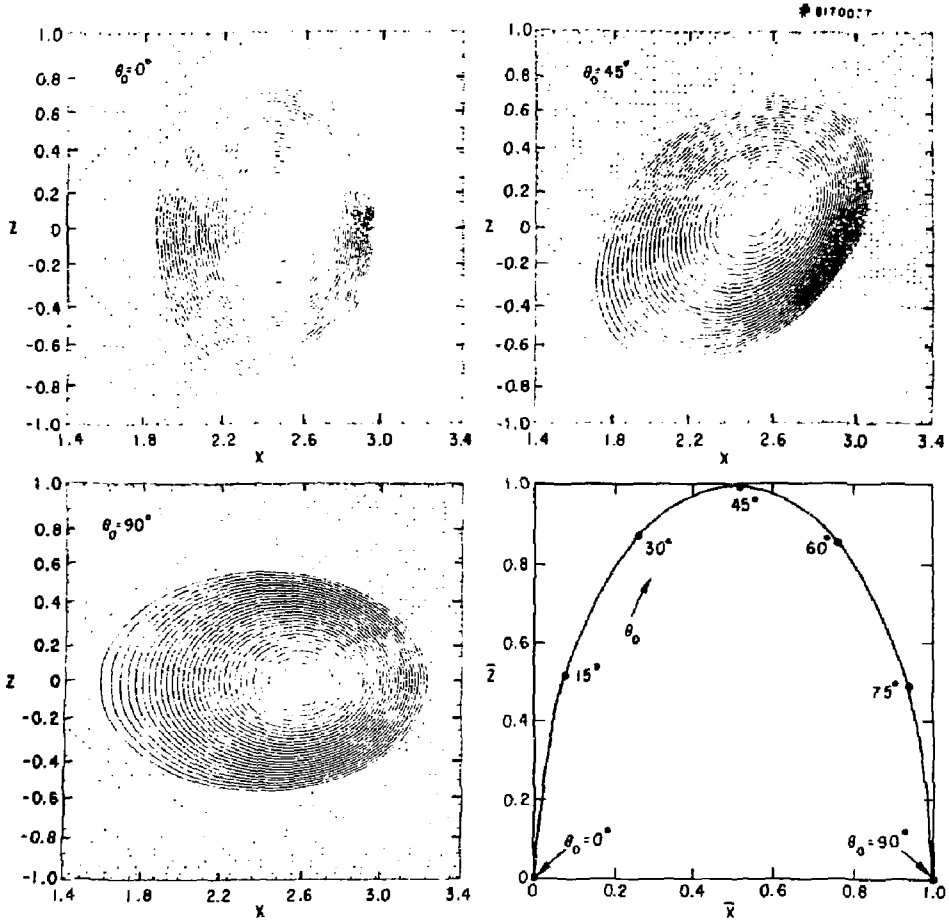
θ0=0°
θ0=45°
θ0=90°
Z
X
1.0
0.8
0.6
0.4
0.2
0
-0.2
-0.4
-0.6
-0.8
-1.0
1.4
1.8
2.2
2.6
3.0
3.4
45°
30°
60°
15°
75°
θ0
θ0=0°
θ0=90°
Z̄
X̄
0
0.2
0.4
0.6
0.8
1.0

Fig. 1.

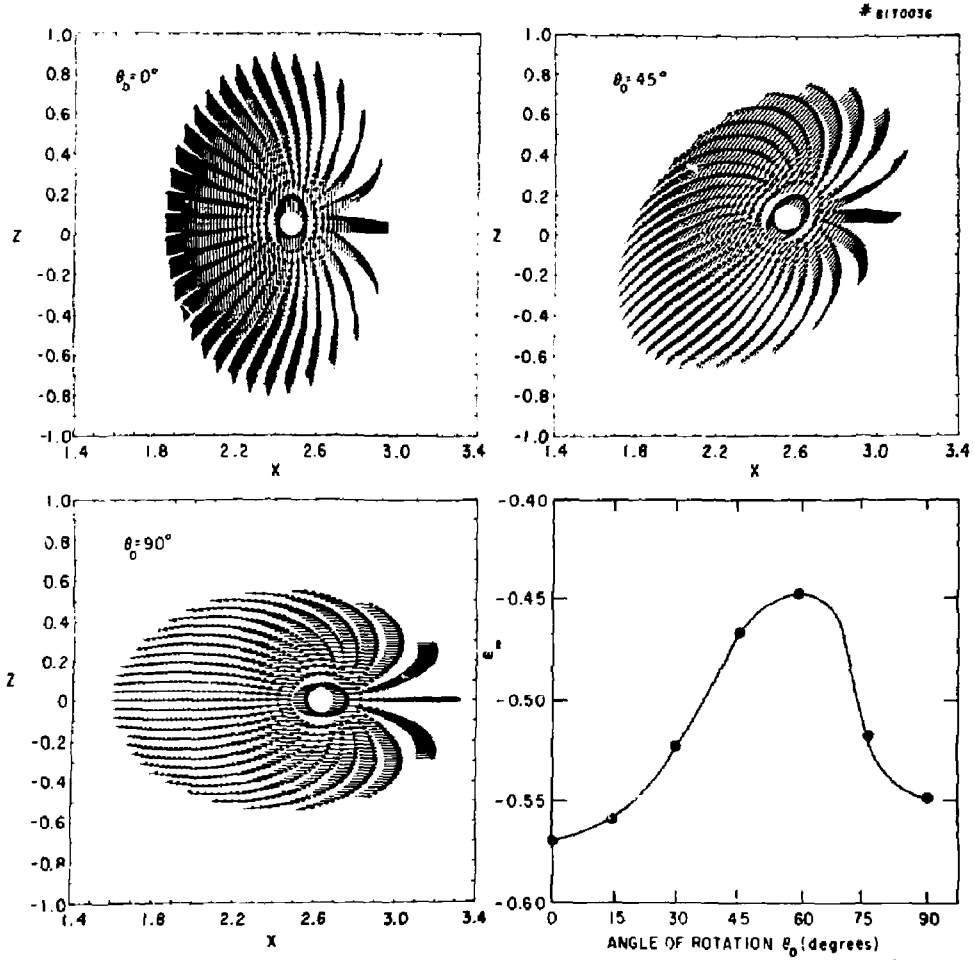
#81T0036
θ0=0°
θ0=45°
θ0=90°
Z
X
1.0
0.8
0.6
0.4
0.2
0
-0.2
-0.4
-0.6
-0.8
-1.0
1.4
1.8
2.2
2.6
3.0
3.4
-0.40
-0.45
-0.50
-0.55
-0.60
0
15
30
45
60
75
90
ANGLE OF ROTATION θ0 (degrees)

Fig. 2.

81T0035

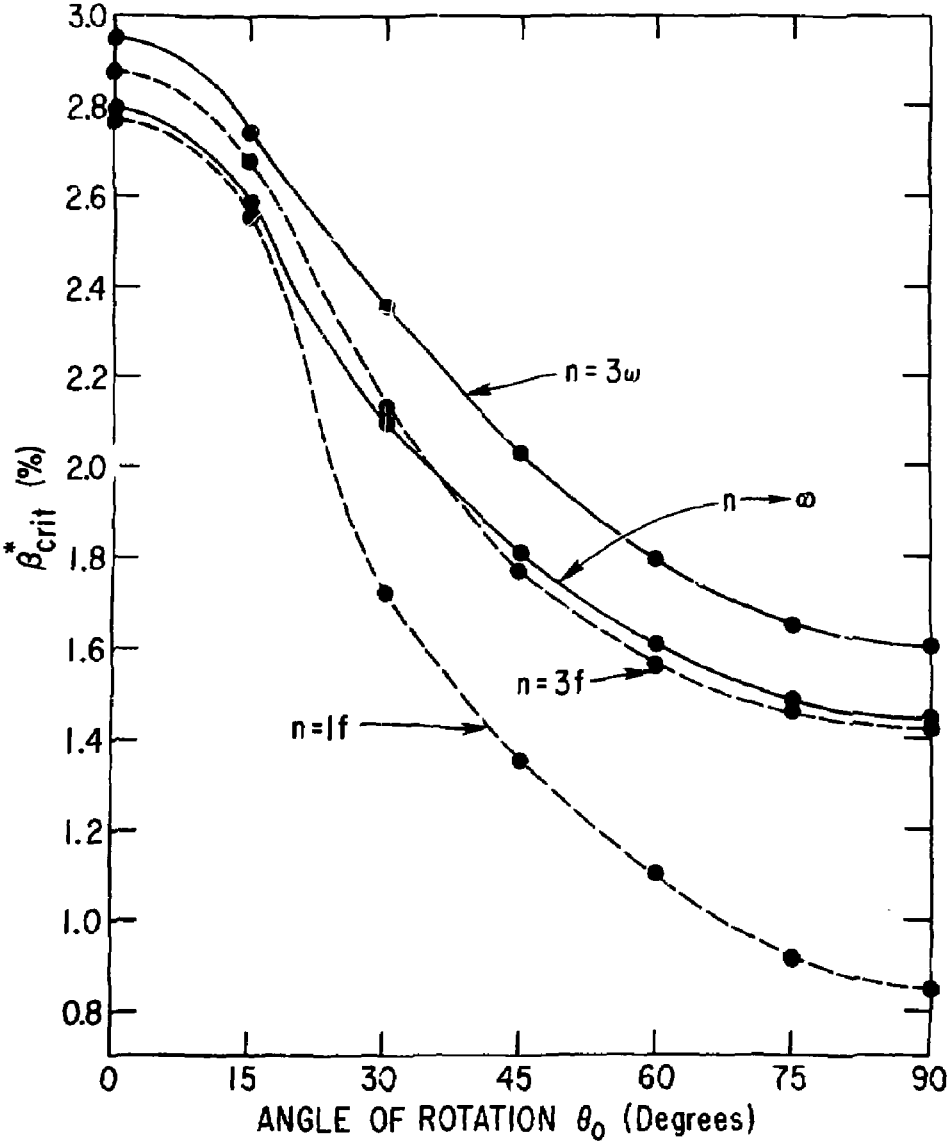

Fig. 3.

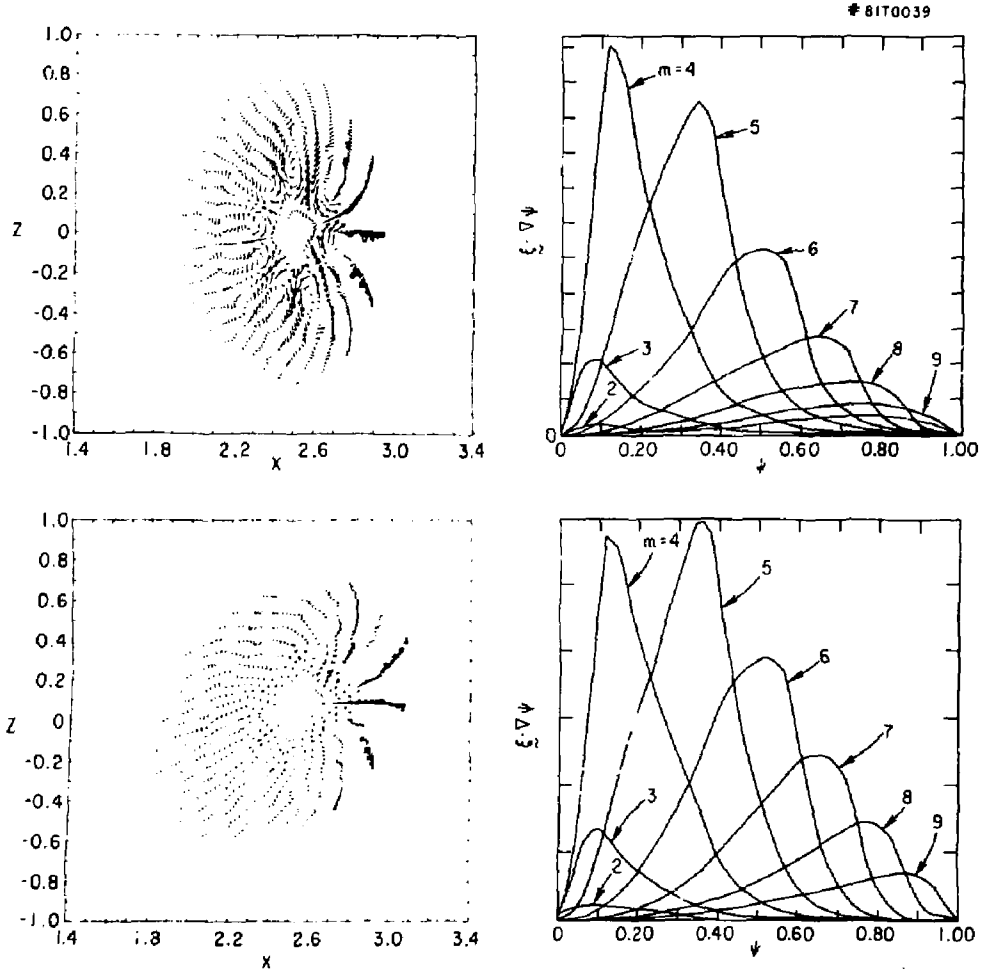
#81T0039
1.0
0.8
0.6
0.4
0.2
Z 0
-0.2
-0.4
-0.6
-0.8
-1.0
1.4
1.8
2.2
2.6
3.0
3.4
X
m=4
5
6
7
8
9
3
2
ξ·∇ψ
0
0.20
0.40
0.60
0.80
1.00
ψ

Fig. 4.

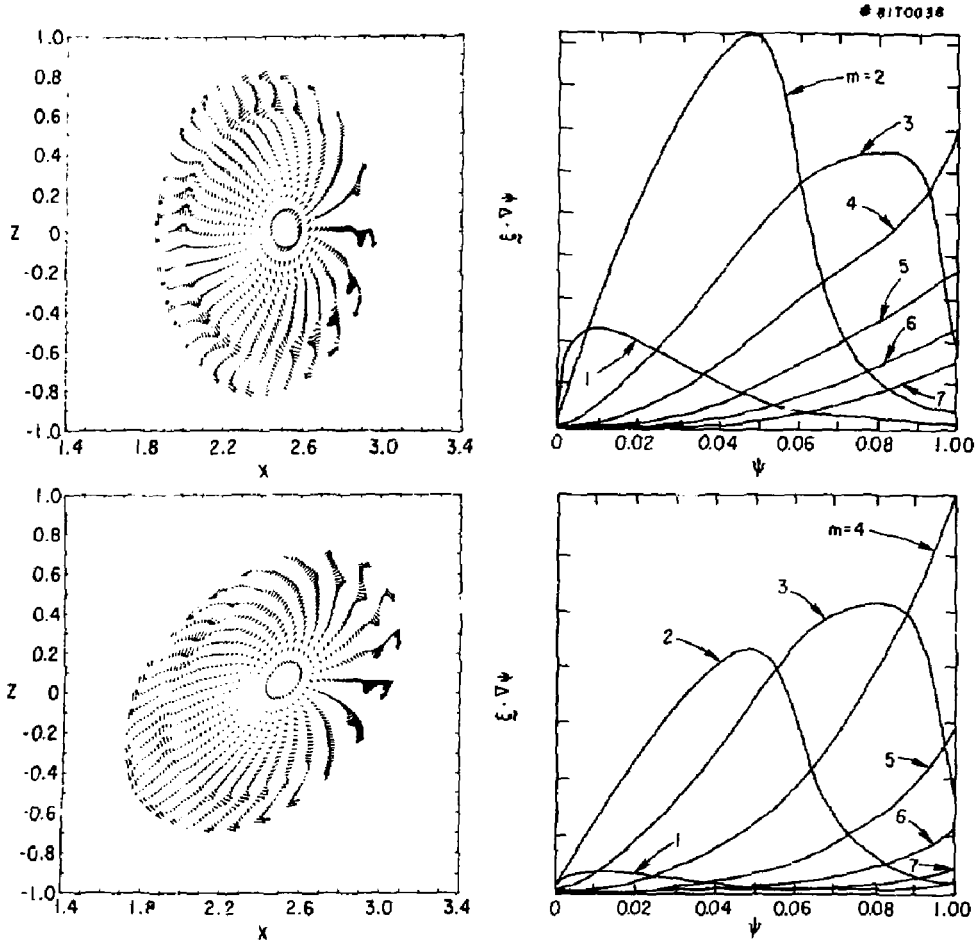

Fig. 5.